

Shot-noise limited monitoring and phase locking of the motion of a single trapped ion

P. Bushev,¹ G. Hétet,^{2,3} L. Slodička,² D. Rotter,² M. A. Wilson,² F. Schmidt-Kaler,⁴ J. Eschner,⁵ and R. Blatt^{2,3}

¹Physikalisches Institut, Karlsruher Institut für Technologie, D-76128 Karlsruhe, Germany

²Institute for Experimental Physics, University of Innsbruck, A-6020 Innsbruck, Austria

³Institute for Quantum Optics and Quantum Information of the Austrian Academy of Sciences, A-6020 Innsbruck, Austria

⁴QUANTUM, Institut für Physik, Universität Mainz, D-55128 Mainz, Germany

⁵Experimentalphysik, Universität des Saarlandes, D-66123 Saarbrücken, Germany

(Dated: December 6, 2012)

We perform high-resolution real-time read-out of the motion of a single trapped and laser-cooled Ba^+ ion. By using an interferometric setup we demonstrate shot-noise limited measurement of thermal oscillations with resolution of 4 times the standard quantum limit. We apply the real-time monitoring for phase control of the ion motion through a feedback loop, suppressing the photon recoil-induced phase diffusion. Due to the spectral narrowing in phase-locked mode, the coherent ion oscillation is measured with resolution of about 0.3 times the standard quantum limit.

The control of a system often relies on gathering information about its evolution in real time, and using it in a feedback loop to drive it into a desired state [1]. In classical physics, the accuracy of such feedback operations can in theory be controlled with infinite precision. In quantum physics, however, there is a fundamental limit to the amount of knowledge one can gain about a system, with important consequences for its controllability [2–5]. If one observes the motion of a body, the uncertainty in a position measurement inevitably arises due to the Heisenberg relation. A measurement of its position disturbs its momentum, leading to an overall blur of the observed motion. The resulting displacement uncertainty is minimized in the so-called “standard measurement procedure” which leads to the standard quantum limit (SQL) [6]. In the case of a harmonic oscillator, the SQL is equal to the position variance of its ground state $\Delta x_{SQL} = \sqrt{\langle 0|r^2|0\rangle} = \sqrt{\hbar/2M\omega}$, where M is the mass of the oscillator and ω its resonant frequency.

Cooling to the quantum mechanical ground state has been demonstrated for elementary harmonic oscillators such as trapped ions [7] and electrons [8], as well as for nanomechanical oscillators [9, 10]. The measurement resolution achieved in experiments with mechanical oscillators of very different sizes typically settles at the level of 5-10 Δx_{SQL} , from the kilogram size oscillator in gravitational wave astronomy in the LIGO experiment [11], down to various nanomechanical systems [12–14]. Only recently, resolution below the standard quantum limit has been demonstrated with nanomechanical oscillators [15, 16]. In experiments measuring the trajectory of a single atom in real time, the resolution achieved so far has remained bounded by a few Δx_{SQL} [17, 18].

In this letter we present high-resolution real-time read-out of the motion of a single trapped and laser-cooled barium ion. The relevant oscillation frequency of one of its macromotion degrees of freedom is $\omega_0/2\pi \sim 1$ MHz, corresponding to a ground state wave function with a spatial extension of $\Delta x_{SQL} \sim 6$ nm. Using an interferometric

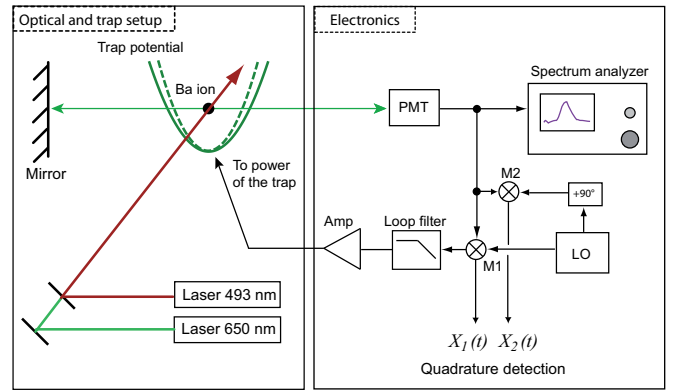


FIG. 1: (Color online) Optical and electronic setup for continuous read-out of ion oscillation and feedback operation. LO denotes local oscillator, PMT stands for photomultiplier (in photon counting mode), M1 and M2 are radio frequency mixers, Amp is an amplifier. The parabola represents the trapping potential confining the ion.

setup [19, 20] we are able to monitor the trajectory of the ion motion with $4\Delta x_{SQL}$ resolution, only limited by the resonance fluorescence noise. We furthermore demonstrate efficient suppression of the photon recoil-induced phase diffusion of the single-ion motion, by phase locking it to an external oscillator. The motion of the locked oscillator is detected with resolution below the SQL.

Figure 1 shows a schematic of the set-up. We use a single $^{138}\text{Ba}^+$ ion which is held in a miniature Paul trap and continuously laser-excited and -cooled on its $S_{1/2}$ to $P_{1/2}$ transition at 493 nm [21]. The ion oscillates in three non-degenerate modes with frequencies of about 1 MHz, 1.2 MHz, and 2 MHz. A retro-reflecting mirror $L = 25$ cm away from the trap and a lens (not shown) are arranged such that they image the ion onto itself. The 493 nm fluorescence of the ion which is scattered directly towards the photomultiplier (PMT) interferes with the part of the fluorescence retro-reflected from the mirror.

Scanning the ion-mirror distance then leads to interference fringes at the position of the PMT with a contrast of up to 73% [19].

For continuous read-out of the ion position, the mirror position is fixed in such a way that the ion stays at the midpoint of the fringes [20]. Then the motion of the ion leads to a modulation of the intensity of the scattered light, i.e. a modulation in the arrival times of the photo-counts. When the signal from the PMT is measured with an RF spectrum analyzer, the motion along the trap axis at frequency $\omega_0 = 2\pi \times 1.039$ MHz appears as a clear resonance line above the shot noise background, as shown in Fig. 2(a). Using a semiclassical picture for the detected light and considering the trapped ion as a point particle oscillating with instantaneous displacement $x(t)$ along the trap axis, the detected photocurrent $i(t)$ is

$$i(t) \propto I_0 [1 + V \sin(2kx(t) \cos \Theta)] + \delta I(t). \quad (1)$$

Here I_0 is the mean fluorescence rate in counts/sec, V is the visibility of the interference fringes limited by imperfect optics and imaging as well as by the motion along other trap axes, k is the wavevector of the 493 nm light, $\Theta = 55^\circ$ is the projection angle between trap axis and optical axis, and $\delta I(t)$ represents the fluorescence shot noise. The single Ba^+ ion is trapped in the Lamb-Dicke regime, therefore Eq. (1) can be rewritten as

$$i(t) \propto I_0 (1 + 2V k x(t) \cos \Theta) + \delta I(t). \quad (2)$$

The spectrum of the photocurrent detected by the RF spectrum analyzer consists of three terms,

$$\langle i^2(\omega) \rangle \propto I_0 + 2\pi I_0^2 \delta(\omega) + 4I_0^2 V^2 k^2 S_x(\omega) \cos^2 \Theta. \quad (3)$$

The first term corresponds to the shot-noise which scales linearly with I_0 , the second one is the DC-offset or mean intensity level which is outside our observation frequency range. The last term reveals the power spectral density of the ion motion, $S_x(\omega)$. It is calculated using the Fluctuation-Dissipation Theorem (FDT) [11, 12, 22, 23] for a harmonic oscillator coupled to a thermal bath with temperature T , which yields

$$S_x(\omega) = \frac{4k_B T \gamma}{M} \cdot \frac{1}{(\omega_0^2 - \omega^2)^2 + \gamma^2 \omega^2}, \quad (4)$$

where M is the mass of the ion and γ is the damping rate of the oscillation. In our case, the measured resonance width $\gamma = 2\pi \times 380$ Hz gives directly the cooling rate of the trapped ion [21]. The area under the resonance curve is proportional to the thermal energy of the oscillator,

$$\langle x^2 \rangle = \frac{1}{2\pi} \int_0^\infty S_x(\omega) d\omega = \int_0^\infty \tilde{S}_x(f) df. \quad (5)$$

To calibrate the power spectral density $\tilde{S}_x(f)$ measured on the spectrum analyzer in terms of displacement, we apply a weak sinusoidal signal to one of the

trap electrodes [24, 25]. This weak excitation is detuned by 2.5 kHz from ω_0 and coherently excites the ion motion, as shown in Fig. 2(a). The relation between the motional amplitude of this coherent oscillation and the spectrum analyzer signal is found by measuring the change of the (time-averaged) fringe contrast at different excitation levels. Using Eq. (1), we then obtain the calibrated spectral density for the ion motion in nm^2/Hz , as shown in Fig. 2(b). The resonance

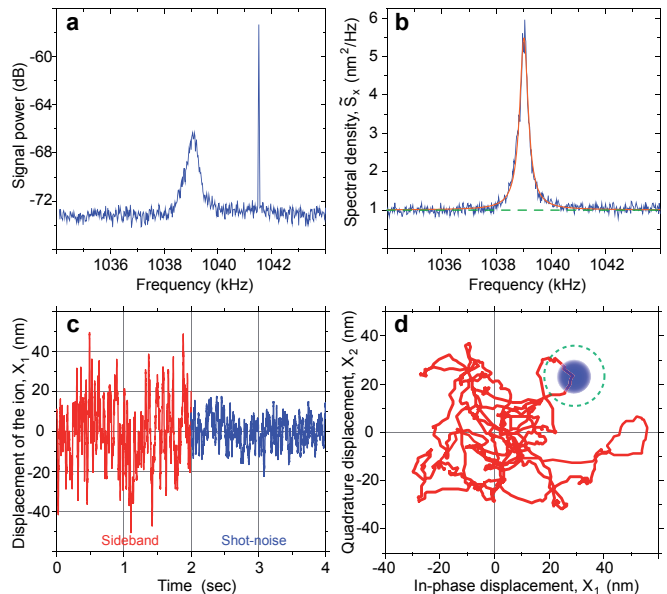


FIG. 2: (Color online) Quantum limited detection of the ion's oscillations. (a) Spectrum of the photocurrent showing motional sideband (wide resonance line) and coherent excitation (sharp peak) used for calibration of the ion's motion. The spectrum was measured with 30 Hz resolution bandwidth (RBW). (b) The blue curve is the calibrated spectral density of the ion displacement $\tilde{S}_x(f)$. The red solid line is a Lorentzian fit, as described by Eq. (4). The precision of the position measurement is set by the shot noise background shown as a dashed green line. (c) Time evolution of the in-phase homodyne signal $X_1(t)$ measured when the local oscillator is tuned in resonance with the ion's oscillation (red curve, $T = 0$ to 2 sec), and when it is tuned off-resonant detecting shot noise only (blue curve, $T = 2$ to 4 sec). The data is smoothed with a 30 Hz low-pass filter, and the sampling rate was $(0.4 \text{ ms})^{-1}$. (d) Phase plot $(X_1, X_2)(t)$ of the motion for 300 ms (red line), using data as in (c). The blue circle shows the uncertainty of any point of the smoothed trajectory due to the shot noise. The green circle shows the resolution of the unsmoothed trajectory as derived from the spectral measurement in (b).

line is well fitted using Eq. (4), which yields through Eq. (5) the mean (r.m.s.) amplitude of the ion excursion $\langle x(t)^2 \rangle^{1/2} = 51$ nm. This value is higher than the one estimated from the Doppler cooling limit, $x_D \approx 27$ nm, set by the linewidth $\Gamma = 2\pi \times 20.4$ MHz of the S to P cooling transition. That is because the laser detunings and intensities chosen to maximize the signal-to-noise ratio

do not provide optimal cooling conditions.

From figure 2(b) we determine the achievable resolution of the position measurement, i.e. the minimum attainable uncertainty of any point of the trajectory when the ion's motion is monitored in real time. It is set by the shot-noise pedestal with spectral density $S_{SN} = 1.0 \text{ nm}^2/\text{Hz}$ shown by the dashed line in Fig. 2(b), and corresponds to an excursion of the ion motion of 24 nm, or $4\Delta x_{SQL}$ [11, 12]. If the oscillation of the ion were aligned with the optical axis, the resolution would be improved by a factor of $\cos\Theta$ to $2.3\Delta x_{SQL}$.

To monitor the ion motion, we employ the homodyne technique depicted in Fig. 1 (see also [26]). Part of the detected PMT signal is mixed with a local oscillator (LO) on two RF-mixers M1 and M2 with $\pi/2$ phase shift between them, and the two outputs are low-pass filtered. The resulting signals $X_1(t)$ and $X_2(t)$ are given by

$$X_i(t) = \int_{-\infty}^t H(t-\eta)x_i(\eta)d\eta, \quad (i = 1, 2), \quad (6)$$

where $x_1(t)$ and $x_2(t)$ are the in-phase and quadrature components of the ion motion (including shot noise), and $H(t-\eta)$ is the time response function of the filter.

A time trace of the X_1 -component, with the LO set on- and off-resonant with the oscillation, is shown in Fig. 2(c). Here a 4-pole filter with ~ 30 Hz cut-off frequency is used that transmits about 10% of the total energy of the sideband; the smoothed trajectory illustrates the method better. The acquisition time resolution is set to 0.4 ms. The measured standard deviations are 15 nm on and 7 nm off resonance. In order to compare them to the oscillator excursion of 51 nm and the resolution of 24 nm as determined from Fig. 2(b), they need to be scaled with the square root of oscillator bandwidth (380 Hz) over filter bandwidth (30 Hz), which leads to very good agreement. A phase plot of the sideband signal, $X_1(t)$ versus $X_2(t)$, is shown during 300 ms in Fig. 2(d), exhibiting photon recoil-induced phase diffusion. The circles indicate the uncertainty on this smoothed trajectory (blue) and the uncertainty for an optimal filter, i.e. the resolution (green).

We now use the homodyne signal in full real-time conditions, i.e. with a low-pass filter that matches the oscillator bandwidth. As an application, we seek to drive the ion motion into a defined coherent state, by phase-locking it to a local oscillator. To this end, the output of mixer M1 is low-pass filtered with 300 Hz cut-off frequency and amplified, thus providing an output proportional to the phase lag between the ion's vibration and the LO. This signal is used to control the intensity of the trap drive in order to change the trap frequency (see Fig. 1), thereby counteracting the phase diffusion due to photon recoils. This operation is reminiscent of a classical phase-locked loop (PLL), whereby the vibration of the single ion plays the role of the voltage-controlled oscillator, synchronized to the phase of the LO reference.

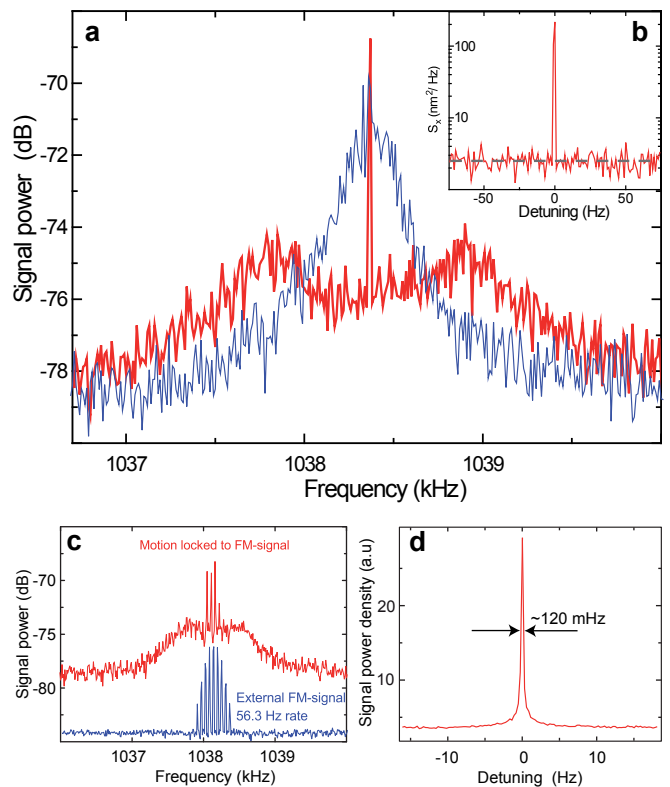


FIG. 3: (Color online) Phase locking of a trapped ion's vibration. (a) Motional sideband spectra when the PLL is off (blue curve) and when the PLL is on (red curve), measured with $\text{RBW} = 10$ Hz. (b) Calibrated spectral density $\tilde{S}_x(f)$ around central peak of phase-locked ion motion, measured with 1 Hz RBW. The dashed line indicates the residual noise floor of $2.6 \text{ nm}^2/\text{Hz}$. (c) Sideband spectrum when the ion is locked to an FM signal with modulation frequency 56.3 Hz and modulation index 1 (red curve). The spectrum of the FM reference is also shown (blue curve). (d) Center peak of phase locked ion motion measured with 50 mHz resolution, using FFT of the $g^{(2)}$ correlation function [27].

To demonstrate the operation of the PLL, the vibrational mode with 1.04 MHz central frequency is first locked to a sinusoidal LO. We show the relevant spectra with and without feedback in Fig. 3(a). Without feedback the sideband spectrum has a Lorentzian shape with about 500 Hz width, determined by the equilibrium between laser cooling and recoil heating. In contrast, with the feedback loop closed, phase locking is clearly observed: the spectrum consists of a narrow central peak and two side-lobes. The peak contains about 1/8 of the total motional energy, and phase noise is suppressed over more than 700 Hz bandwidth, indicating that the ion motion follows the LO closely. The side-lobes indicate the regime where the phase noise is increased, around the oscillation frequency of the feedback loop (servo bumps). The total energy remains constant, i.e. the PLL has no damping effect, in contrast to feedback cooling as in [25]. The coherent, phase locked ion oscillation is detected

with much higher precision than the free thermal motion due to the narrowing of the resonance line and the detection bandwidth. As can be seen from Fig. 3(b), the width of the coherent line is not yet resolved with 1 Hz resolution bandwidth. Using 1 Hz as the upper limit, we find that the coherent motion is detected with better than $0.3\Delta x_{SQL}$ resolution against the residual phase noise pedestal in closed-loop operation: the spectral density of the residual noise of $2.6 \text{ nm}^2/\text{Hz}$ corresponds to motion with 1.6 nm mean excursion.

We demonstrate further the potential of the phase lock by the response to a frequency-modulated (FM) reference, whose spectrum consists of several bands separated by the modulation frequency. Modulation frequency and index are chosen such that the FM harmonics do not coincide with 50 Hz noise, and most of the spectral energy falls into the bandwidth of the loop filter. The resulting spectrum of the motional sideband is displayed in Fig. 3(c), with the spectrum of the LO as reference. The spectrum of ion motion clearly reproduces the three main bands of the FM reference. This measurement shows, in conjunction with Fig. 3(b), that we can encode and decode phase/frequency information into the motion of the single trapped atom with sensitivity below the standard quantum limit.

To resolve the coherent peak in the locked state even better, we use FFT analysis of the second order correlation function $g^{(2)}$, following [27]. Fig. 3(d) shows the central portion of the FFT spectrum, now using 50 mHz resolution. The resulting linewidth of the locked signal is 120 mHz. This residual width is determined mainly by the fact that the time base used in recording $g^{(2)}$ is not synchronized to the 10 MHz clock used for generating the local oscillator. In principle, the narrow linewidth would allow deriving a new limit for the resolution of the ion motion, but calibration proves less reliability for the FFT spectrum than for the one recorded with the rf spectrum analyzer.

In conclusion, we have demonstrated shot-noise limited continuous measurement of the thermal oscillation of a single ion with $4\Delta x_{SQL}$ resolution. The resolution could be moved closer to the standard quantum limit by collecting more fluorescence light, or by introducing a steeper gradient in the interferometric detection of the motion. The first method would employ using a lens with higher numerical aperture [28, 29], the second one may be implemented by setting up the trap inside an optical cavity [30, 31]. We have also realized phase control of the ion motion, suppressing the photon recoil-induced phase diffusion through a PLL-type feedback loop. Due to the narrowing of the resonance line in PLL mode, the coherent ion oscillation is measured with $0.3\Delta x_{SQL}$ resolution.

The measured trajectory of the ion has three noise contributions arising from its ground state motion, the shot-noise of the detected fluorescence, and the recoil back-action of the scattered photons [32]. The latter also

determines the steady state of the motion through the laser cooling process. The PLL control diminishes the shot-noise contribution by narrowing the observed line. The resulting improvement of the displacement resolution does not affect the quantum mechanical part of the trajectory Δx associated with the zero-point motion of the ion, and hence does not influence its momentum uncertainty $\Delta p \simeq \hbar/2\Delta x$. Also the back-action part remains unchanged, since the PLL control stabilizes the phase but does not alter the temperature of the ion.

The potential of the PLL control has been demonstrated by synchronizing the ion's oscillation to a modulated reference signal. The phase locking technique may be used to attain common-mode rejection of recoil effects in photonic atom-atom interactions [33, 34]. It may also be combined with feedback cooling [25] in order to implement combined amplitude and phase control.

This work has been supported by the Austrian Science Fund (SFB15), the European Commission (QUEST, HPRNCT-2000-00121; QUBITS, IST-1999-13021), the Spanish MICINN (QOIT, CSD2006-00019; QNLP, FIS2007-66944), and the "Institut für Quanteninformation GmbH". P. B. and J. E. thank M. Chwalla, M. Aspelmeyer and G. Morigi for stimulating discussions.

-
- [1] N. Wiener, *Cybernetics or the Control and Communication in the Animal and the Machine* (M.I.T and John Wiley and Sons, New York, 1961).
 - [2] H. M. Wiseman and G. J. Milburn, *Quantum measurement and control* (Cambridge University Press, Cambridge, 2010).
 - [3] S. Ashhab and F. Nori, Phys. Rev. A **82**, 062103 (2010).
 - [4] G. G. Gillett, R. B. Dalton, B. P. Lanyon, M. P. Almeida, M. Barbieri, G. J. Pryde, J. L. O'Brien, K. J. Resch, S. D. Bartlett, and A. G. White, Phys. Rev. Lett. **104**, 080503 (2010).
 - [5] C. Sayrin et al., Nature **477**, 73 (2011).
 - [6] B. Braginsky and F. Khalili, *Quantum measurement* (Cambridge University Press, Cambridge, 1999).
 - [7] F. Diedrich, J. C. Bergquist, W. M. Itano, and D. J. Wineland, Phys. Rev. Lett. **62**, 403 (1989).
 - [8] S. Peil and G. Gabrielse, Phys. Rev. Lett. **83**, 1287 (1999).
 - [9] A. D. O'Connell, M. Hofheinz, M. Ansmann, R. C. Bialczak, M. Lenander, E. Lucero, M. Neeley, D. Sank, H. Wang, M. Weides, et al., Nature **464**, 697 (2010).
 - [10] J. Chan, T. P. M. Alegre, A. H. Safavi-Naeini, J. T. Hill, A. Krause, S. Gröblacher, M. Aspelmeyer, and O. Painter, Nature **478**, 89 (2011).
 - [11] B. Abbott and others (LIGO Scientific Collaboration), New J. Phys. **11**, 073032 (2009).
 - [12] M. LaHaye, O. Buu, B. Camarota, and K. Schwab, Science **304**, 74 (2004).
 - [13] S. Gröblacher, J. B. Hertzberg, M. R. Vanner, S. Gigan, K. C. Schwab, and M. Aspelmeyer, Nature Physics **5**, 485 (2009).
 - [14] P. Verlot, A. Tavernarakis, T. Briant, P.-F. Cohadon,

- and A. Heidmann, Phys. Rev. Lett. **104**, 133602 (2010).
- [15] J. D. Teufel, T. Donner, M. A. Castellanos-Beltran, J. W. Harlow, and K. W. Lehnert, Nature Nanotechnology **4**, 820 (2009).
- [16] G. Anetsberger, E. Gavartin, O. Arcizet, Q. P. Unterreithmeier, E. M. Weig, M. L. Gorodetsky, J. P. Kotthaus, and T. J. Kippenberg, Phys. Rev. A **82**, 061804(R) (2010).
- [17] C. J. Hood, T. W. Lynn, A. C. Doherty, A. S. Parkins, and H. J. Kimble, Science **287**, 1457 (2000).
- [18] P. W. H. Pinkse, T. Fischer, P. Maunz, and G. Rempe, Nature **404**, 365 (2000).
- [19] J. Eschner, C. Raab, F. Schmidt-Kaler, and R. Blatt, Nature **413**, 495 (2001).
- [20] P. Bushev, A. Wilson, J. Eschner, C. Raab, F. Schmidt-Kaler, C. Becher, and R. Blatt, Phys. Rev. Lett. **92**, 223602 (2004).
- [21] C. Raab, J. Eschner, J. Bolle, H. Oberst, F. Schmidt-Kaler, and R. Blatt, Phys. Rev. Lett. **85**, 538 (2000).
- [22] H. B. Callen and T. A. Welton, Phys. Rev. **83**, 34 (1951).
- [23] M. Pinard, P. F. Cohadon, T. Briant, and A. Heidmann, Phys. Rev. A **63**, 013808 (2000).
- [24] P. Bushev, *PhD Thesis* (Innsbruck University, 2004).
- [25] P. Bushev, D. Rotter, A. Wilson, F. Dubin, C. Becher, J. Eschner, R. Blatt, V. Steixner, P. Rabl, and P. Zoller, Phys. Rev. Lett. **96**, 043003 (2006).
- [26] T. Briant, P. F. Cohadon, M. Pinard, and A. Heidmann, Eur. Phys. J. D **22**, 131 (2003).
- [27] D. Rotter, M. Mukherjee, F. Dubin, and R. Blatt, New J. Phys. **10**, 043011 (2008).
- [28] M. Sondermann, R. Maiwald, H. Konermann, N. Lindlein, U. Peschel, and G. Leuchs, Applied Physics B: Lasers and Optics **89**, 489 (2007).
- [29] E. W. Streed, B. G. Norton, A. Jechow, T. J. Weinhold, and D. Kielpinski, Phys. Rev. Lett. **106**, 010502 (2011).
- [30] G. R. Guthöhrlein, M. Keller, K. Hayasaka, W. Lange, and H. Walther, Nature **414**, 49 (2001).
- [31] A. B. Mundt, A. Kreuter, C. Becher, D. Leibfried, J. Eschner, F. Schmidt-Kaler, and R. Blatt, Phys. Rev. Lett. **89**, 103001 (2002).
- [32] K. Jacobs, I. Tuttonen, H. M. Wiseman, and S. Schiller, Phys. Rev. A **60**, 538 (1999).
- [33] C. Cabrillo, J. I. Cirac, P. García-Fernández, and P. Zoller, Phys. Rev. A **59**, 1025 (1999).
- [34] S. Rist, J. Eschner, M. Hennrich, and G. Morigi, Phys. Rev. A **78**, 013808 (2008).